A New Method Based on Extension Theory for Partial Discharge Pattern Recognition

HUNG-CHENG CHEN, FENG-CHANG GU, and CHUN-YAO LEE*
Department of Electrical Engineering
National Chin-Yi University of Technology
35, Lane 215, Sec. 1, Chungshan Road, Taiping, Taichung, Taiwan
hcchen@ncut.edu.tw, biobhst@hotmail.com
*Department of Electrical Engineering
Chung Yuan Christian University
200, Chung Pei Road, Chung Li, Taiwan
cyl@cycu.edu.tw

Abstract: - This paper proposes a new partial discharge (PD) pattern recognition method base on the extension theory. First, five types of defect models are well-designed on the base of investigation of many power equipment failures. A commercial PD detector is used to measure the three-dimension (3D) PD patterns, then two fractal features (fractal dimension and lacunarity) and mean discharges of phase windows are extracted from the raw 3D PD patterns. Second, the matter-element models of the PD defect types are built according to the PD features derived from practical experimental results. The PD defect type can be directly identified by correlation degrees between the tested pattern and the matter-element models. To demonstrate the effectiveness of the proposed method, comparative studies using a multilayer neural network (MNN) are conducted on 200 sets of field-test PD patterns with rather encouraging results.

Key-Words: - Extension Theory, Partial Discharge, Pattern Recognition.

1 Introduction

Partial discharge (PD) measurement has been widely application in insulation diagnosis for power equipment. It is an important tool for power apparatus, such as XLPE power cable [1], gas insulation switch and power transformers diagnosis. The main purpose of insulation diagnosis for power apparatus is to give system operators the information on dielectric deterioration degree of HV equipment. Using commercial PD detectors can measure the electrical signal of electrical or magnetic field variety in defect model, and an experienced expert can use the PD patterns to identify the defect types in the tested object. The main parameters of the 3D PD patterns are phase angle ϕ, discharge magnitude q, and the numbers of discharge n.

Fractal has been very successfully used in description of naturally occurring phenomena and complex shape [2], [3], such as mountain ranges, coastlines, clouds, and so on, wherein traditional mathematical were found to be inadequate. PD also is a natural phenomenon occurring in electrical insulation systems, which invariably contain tiny defects and non-uniformities, and gives rise to a variety of complex shapes and surfaces, both in a physical sense as well as in the shape of 3D PD patterns acquired using digital PD detector. This complex nature of the PD pattern shapes and the ability of fractal geometry to model complex shapes, is the main reason which encouraged the authors to make an attempt to study its feasibility for PD pattern interpretation.

Various pattern recognition techniques, including fuzzy clustering [4], [5], and neural network (NN) [6], [7], have been extensively used in PD recognition. The main advantage of a MNN can directly acquire experience from the training data. However, the training data must be sufficient to describe a status. Another limitation of the MNN approach is the inability to use linguistic describe output, because it is difficult to understand the content of network. To overcome the limitation of the MNN mentioned above, a new PD recognition method base on extension theory is proposed for classifing PD defect model in this paper. The extension theory was first proposed by Cai Wen to solve contradictions and incompatibility problems in 1983 [8]. Extension theory consists of matter-element model and extended set theory. It does not require particular learning processes and artificial parameters. To demonstrate the effectiveness of the extension recognition method, 200 sets of PD patterns are tested. The results show that the extension recognition method is suitable as a practical solution.

2 Outline of Extension Theory

Extension theory concepts contain the matter-elements and extension sets. The main purpose of extension theory is to solve contradiction and incompatibility problems. The matter-element can easily represent the nature of matter. The extension set is the quantitative tool of extension theory. It can represent the correlation degree of the matter-element by designed correlation function. Some definitions of extension theory are introduced in the following [8]:

2.1 Matter-Element Theory

In extension theory, a matter-element uses an ordered triad for describing things as

$$R = (T, c, v) \tag{1}$$

where T represents the matter, c represents the characteristic, v represents the measure of the characteristics c. If we assume that $C = (c_1, c_2, \cdots, c_n)$ is a characteristics vector and $V = (v_1, v_2, \cdots, v_n)$ is a value vector of C. Then multidimensional matter-element can define as

$$R = (T, C, V) = \begin{bmatrix} R_1 \\ R_2 \\ \vdots \\ R_n \end{bmatrix} = \begin{bmatrix} T & c_1 & v_1 \\ & c_1 & v_2 \\ & \vdots & \vdots \\ & c_n & v_n \end{bmatrix} \tag{2}$$

where $R_i = (T, c_i, v_i)$ $(i = 1, 2, \cdots, n)$ is defined as the submatter-element of R. For example

$$R = \begin{bmatrix} \textit{ball A} & \textit{weight} & 100g \\ & \textit{radius} & 10\text{cm} \end{bmatrix} \tag{3}$$

It can be used to state that ball A weight is 100g, and radius is 10cm. Matter has many characteristics and one characteristic or one characteristic element can be proposed by many matters, etc. The base formulations in extension theory can be expressed as follows [8]:

Nature 1: A matter has many characteristics, expressed as

$$(T, c, v) \dashv \{(T, c_1, v_1), (T, c_2, v_2), \cdots, (T, c_n, v_n)\} \tag{4}$$

It shows that matter T can have characteristics $c_1, c_2, \cdots c_n$. The symbol " $\dashv$ " indicates the extension.

Nature 2: One characteristic proposed by many matters, called one characteristic many matters, expressed as

$$(T, c, v) \dashv \{(T_1, c_1, v_1), (T_2, c_2, v_2), \cdots, (T_n, c_n, v_n)\} \tag{5}$$

Nature 3: One characteristic-element can be proposed by many matters, expressed as

$$(T, c, v) \dashv \{(T_1, c_1, v), (T_2, c_2, v), \cdots, (T_n, c_n, v)\} \tag{6}$$

Using the matter-element, we can describes quality and quantity for a matter, which is a new concept theory compared with conventional mathmatics.

2.2 Extension Set

Set theory is a kind of mathematical scheme that describes the classification about an object. The membership function of traditional fuzzy set describes value of matter at interval [0, 1]. The extension set extends the fuzzy set from [0, 1] to $[-\infty, \infty]$. As a result, it allows us to define a set that includes any data in the domain. An extension set is composed two definition as follows [8]:

Definition 1: Let U be a space of objects and x an element of U, then extension set $\tilde{E}$ in U is defined as

$$\tilde{E} = \{(x, y) | x \in U, y = K(x) \in (-\infty, \infty)\} \tag{7}$$

where $y = k(x)$ is called the correlation function for extension set $\tilde{E}$. The $K(x)$ describes level between $-\infty$ to ∞ for each element. An extension set $\tilde{E}$ in U can be denoted by

$$\tilde{E} = E^+ \bigcup Z_0 \bigcup E^- \tag{8}$$

where

$$E^+ = \{(x, y) | x \in U, y = K(x) > 0\} \tag{9}$$

$$E^- = \{(x, y) | x \in U, y = K(x) < 0\} \tag{10}$$

$$Z_0 = \{(x, y) | x \in U, y = K(x) = 0\} \tag{11}$$

E^+ represents $y = k(x) > 0$ the positive field. E^- represents $y = K(x) < 0$ the negative field. Z_0 represents $y = K(x) = 0$ the zero boundary.

Defintion 2: If $X_0 = [a, b]$ and $X_0 = [f, g]$ are two intervals in the real number field, and $X_0 \subset X$, where X_0 and X are the classical and neighborhood domains, respectively. The correlation function in the extension theory can be defined as

$$K(x) = \begin{cases} \dfrac{-2\rho(x, X_0)}{b - a}, & x \in X_o \\ \dfrac{\rho(x, X_0)}{\rho(x, X) - \rho(x, X_0)} & x \notin X_0 \end{cases} \tag{12}$$

where

$$\rho(x, X_0) = \left| x - \frac{a + b}{2} \right| - \frac{b - a}{2} \tag{13}$$

$$\rho(x, X) = \left| x - \frac{f + g}{2} \right| - \frac{g - f}{2} \tag{14}$$

The correlation function can calculate the membership grade between x and X_0. The extension correlation function concept is shown in Fig.1. When $K(x) \geq 0$, it means x in the interval [a,b]. When $K(x) < 0$, it describes x does not belong to X_0. When $-1 < K(x) < 0$, it is called the extension domain, which means that the element still has a chance to become part of the set if conditions change.

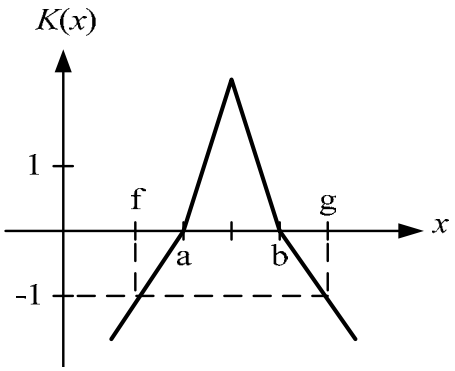

Fig.1 Extension membership function

3 Extraction of PD Features

Fractals have been very successfully used to address the problem of modeling and to provide a description of naturally occurring phenomena and shapes, wherein conventional and existing mathematical methods were found to be inadequate. In recent years, this technique has increased attention for classification of textures and objects present in images and natural scenes [9], and for modeling complex physical processes. In this theory, fractal dimensions are allowed to depict surface asperity of complicated geometric things. Therefore, it is possible to study complex objects with simplified formulas and fewer parameters [10]. PD also is a natural phenomenon occurring in electrical insulation systems, which invariably contain tiny defects and non-uniformities, and gives rise to a variety of complex shapes and surfaces, both in a physical sense as well as in the shape of 3D PD patterns acquired using digital PD detector. This complex nature of the PD pattern shapes and the ability of fractal geometry to model complex shapes, is the main reason which encouraged the authors to make an attempt to study its feasibility for PD pattern interpretation.

The fractal features, fractal dimension and lacunarity, and the mean discharges of phase windows are extracted to highlight the more detailed characteristics of the raw 3D PD patterns. The extracted features in this paper are introduced as follows:

3.1 Fractal Dimension (Input Parameter 1)

While the definition of fractal dimension by self-similarity is straightforward, it is often difficult to estimate/compute for a given image data. However, a related measure of fractal dimension, the box dimension, can be computed more easily. In this work, the method suggested by Voss, and others in [9], [11], for the computation of fractal dimension *D* from the image data has been followed. Let *p*(*m*,*L*) define the probability that there are *m* points within a box of size *L* (i.e. cube of side *L)*, which is centered about a point on the image surface. *P*(*m*,*L*) is normalized, as below, for all *L*.

$$\sum_{m=1}^{N} p(m,L) = 1 \tag{15}$$

where *N* is the number of possible points within the box. Let *S* be the number of image points (i.e. pixels in an image). If one overlays the image with boxes of side *L*, then the number of boxes with *m* points inside the box is (*S*/*m*)*p*(*m*,*L*). Therefore, the expected total number of boxes needed to cover the whole image is

$$N(L) = \sum_{m=1}^{N} \frac{S}{m} p(m,L) = S \sum_{m=1}^{N} \frac{1}{m} p(m,L) \tag{16}$$

this value is also proportional to L^{-D} and the box dimension can be estimated by calculating $p(m,L)$ and $N(L)$ for various values of *L*, and by doing a least square fit on $[\log(L), \log(N(L))]$. To estimate $p(m,L)$, one must center the cube of size *L* around an image point and count the number of neighboring points *m*, that fall within the cube. Accumulating the occurrences of each number of neighboring points over the image gives the frequency of occurrence of *m*. This is normalized to obtain $p(m,L)$. Values of *L* are chosen to be odd to simplify the centering process. Also, the centering and counting activity is restricted to pixels having all their neighbors inside the image. This will obviously leave out image portions of width $=(L-1)/2$ on the borders. This reduced image is then considered for the counting process. As is seen, large values of *L* results in increased image areas from being excluded during the counting process, thereby increasing uncertainty about counts near border areas of the image. This is one of the sources of errors for the estimation of $p(m,L)$ and thereby *D*. Additionally, the computation time grows with the *L* value. Hence, *L* = 3, 5, 7, and 11 were chosen for this work. Fig.2 shows a sample plot of the set $[\log(L), -\log(N(L))]$ for the different size *L*.

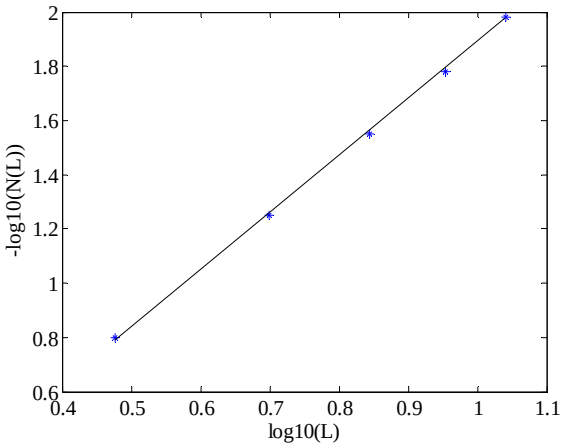

Fig.2 The sample plot of the set $[\log(L), \log(N(L))]$ for different box size L

3.2 Lacunarity (Input Parameter 2)

Theoretically, ideal fractal could confirm to statistical similarity for all scales. In other words, fractal dimensions are independent of scales. However, it has been observed that fractal dimension alone is insufficient for purposes of discrimination, since two differently appearing surfaces could have the same value of *D*. To overcome this, Mandelbrot introduced the term called lacunarity Λ, which quantifies the denseness of an image surface. Many definitions of this term have been proposed and the basic idea in all these is to quantify the 'gaps or lacunae' present in a given surface. One of the useful definitions of this term as suggested by Mandelbrot [l2] is

$$M(L) = \sum_{m=1}^{N} mp(m, L) \tag{17}$$

$$M^2(L) = \sum_{m=1}^{N} m^2 p(m, L) \tag{18}$$

where *N* is the numbers of point in the data set of size *L*, the lacunarity becomes

$$\Lambda(L) = \frac{M^2(L) - [M(L)]^2}{[M(L)]^2} \tag{19}$$

Fig.3 shows a sample plot of the variation of lacunarity with respect to box size *L*(3, 5, 7 ,9 and 11). Fig.4 shows the overall procedure for extracting fractal features. In fractal dimension computation, the first step is to transfer PD pattern to a 512×512 gray scale image matrix. Using different box size *L*, we can obtain *N*(*L*). Finally, fitting the data $\{\log L, -\log(N(L))\}$ can obtain the fractal dimension.

In lacunarity computation, the first step is also to transfer PD pattern to a 512×512 binary image matrix. Then different box size *L* is chosen. *L*=3 is the best box size for the computation of the $M(L)$ and $M^2(L)$. Finally we can obtain lacunarity using equation (18).

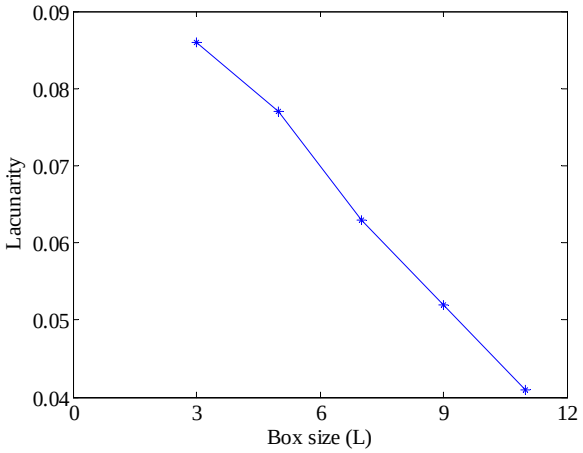

Fig.3 The sample plot of the variation of lacunarity with respect to box size *L*

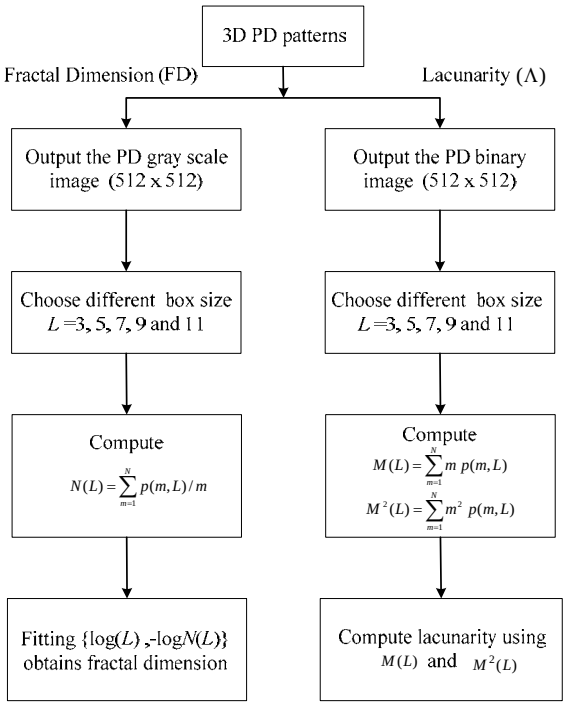

Fig.4 Procedure for computing fractal dimension and lacunarity

3.3 Mean Values of Discharges (Input Parameter 3~12)

The mean discharge is calculated in every phase window which is set to 36°. We will get 10 mean discharge parameters in 360°. If each phase window is devided into $n \times m$ matrix, the mean value of each phase can be calculated by

$$v_i = \frac{\sum_{j=1}^{m}\sum_{k=1}^{n} q_j n_{jk}}{\sum_{j=1}^{m}\sum_{k=1}^{n} n_{jk}} \qquad for\ i = 1, 2, \cdots, 10 \qquad (20)$$

4 PD Recognition System Design

The block diagram of the designed PD recognition system is shown in Fig.5. It consists of three main parts: the well-designed defect models, the measurement system, and the PD extension recognition method. We will introduce the details of the three main parts in subsequent paragraphs.

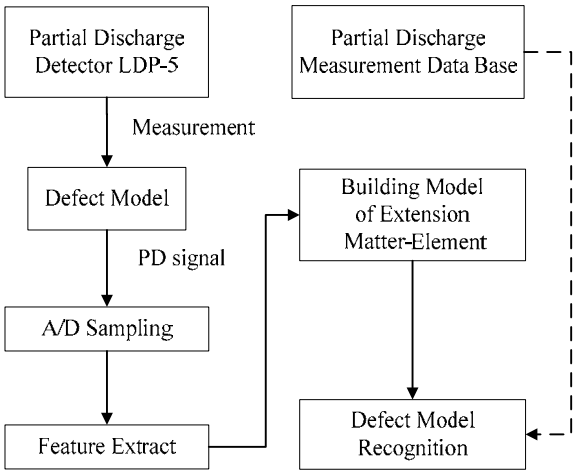

Fig.5 The block diagram of the designed PD recognition system

4.1 Defect Models

According to the fact that gap discharge and surface discharge are more likely to occure in high-voltage power equipments, five types of relevent models are well-designed on the base of investigation of many power equipment failures to outline the features of PD.

T1: Plane to plane model. A 9 mm-in-thickness epoxy with a 3 mm-in-diameter cylindrical cavity is inserted.

T2: Plane to plane model. A 3 mm-in-thickness epoxy is inserted.

T3: Needle to plane model. A 10 mm-in-diameter copper stick is lathed at one end to a 30° 0.5 mm-in-diameter cone needle which is 6 cm away from the plane.

T4: Needle to plane model. A 10 mm-in-diameter copper stick is lathed at one end to a 30° 1 mm-in-diameter cone needle which is 6 cm away from the plane.

T5: Needle to plane model. A 10 mm-in-diameter copper stick is lathed at one end to a 30° 2 mm-in-diameter cone needle which is 6 cm away from the plane.

Both the plane and the needle are made of copper. The practical specimens of the defect models are shown in Fig.6.

Fig.6 The practical specimens of the defect models

4.2 Measurement System

The structure of the measuring system is shown in Fig.7. The autotransformer is used to slowly rise the output voltage of the transformer to 5.4kV as the testing voltage on defect model. The detector LDP-5 with a capacitive sensor measures the PD electrical signal generated by the defect model. The PD signal is converted into a computer by NI DAQ card (PCI-6110) for further analysis. For each type of defect model, 40 times measurement are conducted. The sampling rate of the PCI-6110 DAQ card is set to $2M/s$ and data acquisition duration per measurement is 24 cycles (60Hz). The acquired PD signal is transferred into a 3D pattern. The features of the 3D pattern are extracted and used as the input parameters of the recognition system base on extension recognition method.

A man-machine interface for PD measurement is designed using LabVIEW. Analyzing the signal through LabVIEW can not only obtain the instant

values of PD signal, but also compare to the testing voltage (60Hz) in real time. The designed measurement man-machine interface is shown in Fig.8. The red and green curves indicate the PD signal and the testing voltage waveform, respectively.

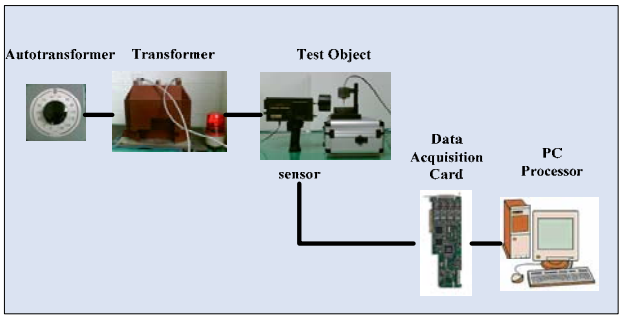

Fig.7 The structure of the measurement system

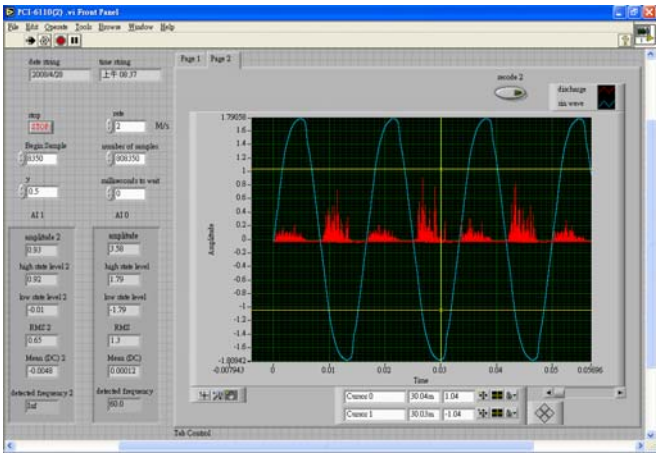

Fig.8 The designed man-machine interface for PD measurement

The detector LDP-5 with a capacitive sensor is used to measure the PD signal of defect model. The typical PD impulse is shown in Fig.9. The rise time is much faster than fall time. The frequency of the impulse is about 20kHz~40kHz.

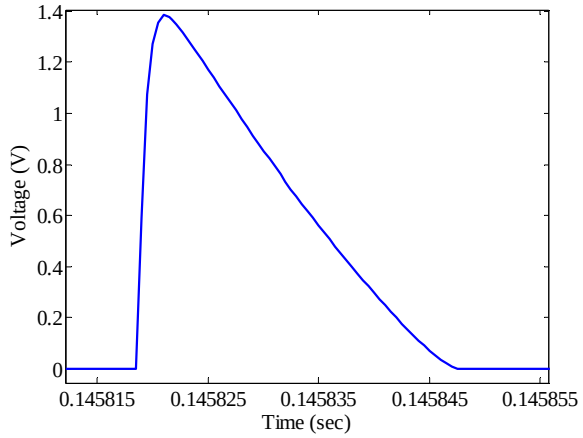

Fig.9 The typical PD impulse

4.3 Extension Recognition Method

The flow chart of the recognition method based on extension theory is shown in Fig.10. The proposed extension recognition method is described as follows:

Step 1: Formulate the matter-element R_i for each defect type as

$$R_i = (T_i, C_j, V_j)$$

$$= \begin{Bmatrix} T_i & c_1 & \langle a_{i1}, b_{i1} \rangle \\ & c_2 & \langle a_{i2}, b_{i2} \rangle \\ & \vdots & \vdots \\ & c_{12} & \langle a_{i12}, b_{i12} \rangle \end{Bmatrix} \quad (21)$$

where

T_i : ith defect type of PD pattern $(i = 1,2,\cdots,5)$

C_j : jth input feature $(j = 1,2,\cdots,12)$.

a_{ij} : low-bounds value of classical domains in the jth input feature for ith defect type.

b_{ij} : up-bounds value of classical domains in the jth input feature for ith defect type.

The ranges of classical domain $V = \langle a, b \rangle$ of each value can directly obtained from the low-bounds and up-bounds of field-test records. Then the neighborhood domain $\hat{V} = \langle f, g \rangle$ of classical domains, the possible range values of each characteristic can be determined. We are set $f = 0.87 \times a$ and $g = 1.13 \times b$.

Step 2: Calculate the degree of correlation for each defect type using equation (12).

Step 3: Set the weights $W_1, W_2, \cdots, W_{12}$ of each feature. We set the weights of both the fractal dimension and the lacunarity at 0.15, the others at 0.07.

Step 4: Calculate the index of correlation for each defect type

$$\zeta_i = \sum_{j=1}^{12} W_j K_{ij} \qquad i = 1,2,\cdots,5 \quad (22)$$

Step 5: Normalize the index of correlation between [-1,1] as equation (16). It will be benefic for fault diagnosis [13].

$$\lambda_i = \frac{2\zeta_i - \zeta_{\min} - \zeta_{\max}}{\zeta_{\max} - \zeta_{\min}} \qquad i = 1,2,\cdots,5 \quad (23)$$

where

$$\zeta_{\max} = \max_{1 \le i \le 5} \{\zeta_i\} \quad (24)$$

$$\zeta_{\min} = \min_{1\le i\le 5}\{\zeta_i\} \quad (25)$$

Step 6: Find the maximum index of correlation. The defect recognition rule is shown as follows:

IF $(\lambda_k = 1)$ THEN $(T_t = T_k)$ (26)

Equation (26) expresses that if $\lambda_k = 1$, then the defect type of this tested model is *k*th defect type.

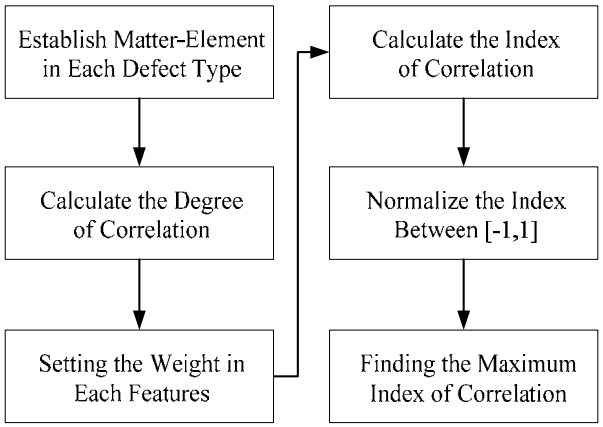

Fig.10 The flow chart of the extension recognition method

5 Experiment Results and Discussions

The proposed extension recognition method has beeen implemented according to the measured PD pattern on the defect models. There is a total of 200 sets of measurement data associatd with the five types of defect models. Some experiment rsults are shown as follows:

5.1 3D PD Patterns

The typical 3D PD patterns transferrd from the measured PD signals for each defect model are shown in Fig.11. The main parameters of the 3D PD patterns are phase angle ϕ, discharge magnitude q, and the numbers of discharge n. We can observe that the number of discharge in type T1 is less then in type T2, but distribution is wider than type T2. It's also very obvious that the numbers of discharge in types T3, T4, and T5 are greater than types T1 and T2. The discharges are happened more frequent when the needle-tip is thinner. The discharges of needle to plane model are almost happened in positive period. Sometimes types T3 and T4 have discharges happened in negative period, in which the number of discharge is few, but the discharge magnitude is large. According to the 3D PD pattern in each defect model we can find some different features between every defect model.

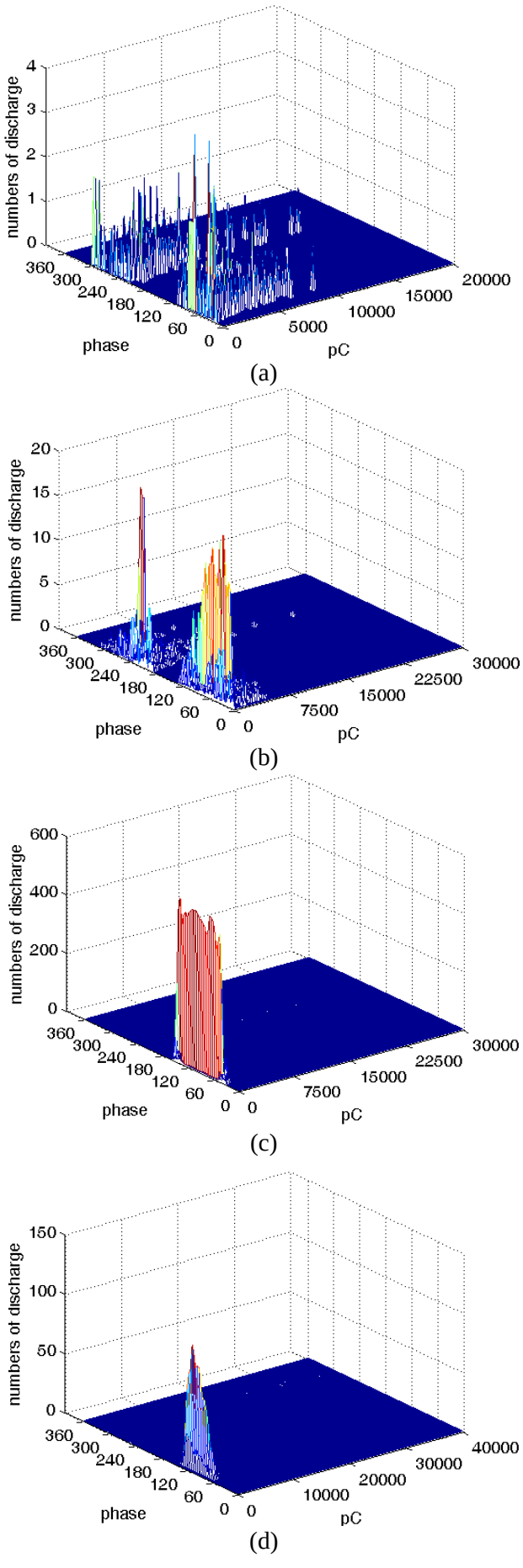

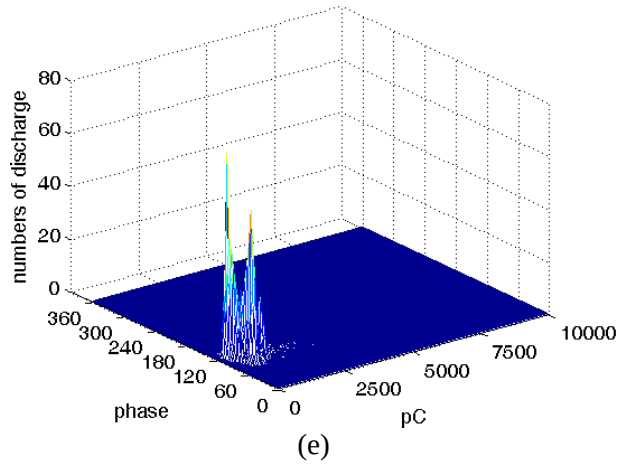

(e)

Fig.11 Five typical defect type of 3D PD patterns. (a) type T1 (b) type T2 (c) type T3 (d) type T4 (e) type T5

5.2 Feature Extraction

The features of a total of 200 sets of 3D PD patterns are extracted and used as the input parameters of the recognition system base on extension recognition method. Two features, the fractal dimension and the lacunarity, are calculated based on the fractal theory. The distribution of the fractal dimension and the lacunarity of all 3D PD patterns is shown in Fig.12. It is obvious that patterns belonging to a particular defect type gather together. According to these two fractal features tyep T1 and type T2 can be easily classified. However, the distribution of type T3, T4, and T5 overlaps somewhere, which causes inaccurate classification. Therefore we take the mean values of discharge associated with phase windows as additional features. The mean discharges of all type of defect models associated with phase windows are shown in Fig.13. We can find out T1 mean discharge is distribution wider than each other. T4 in phase window six to nine is the max discharge than others. In Fig.13 we can notice some differences among all the five defect type models.

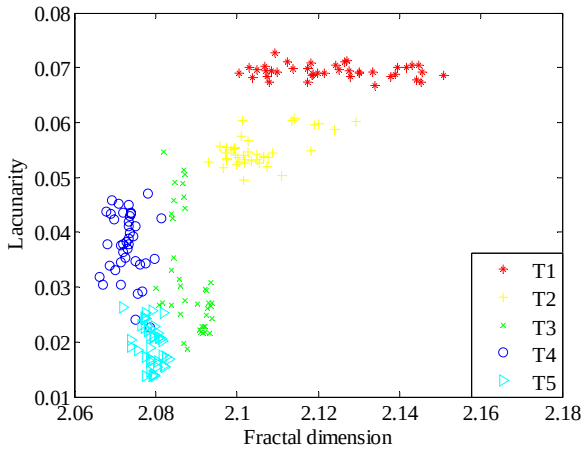

Fig.12 Distribution of fractal features of all models

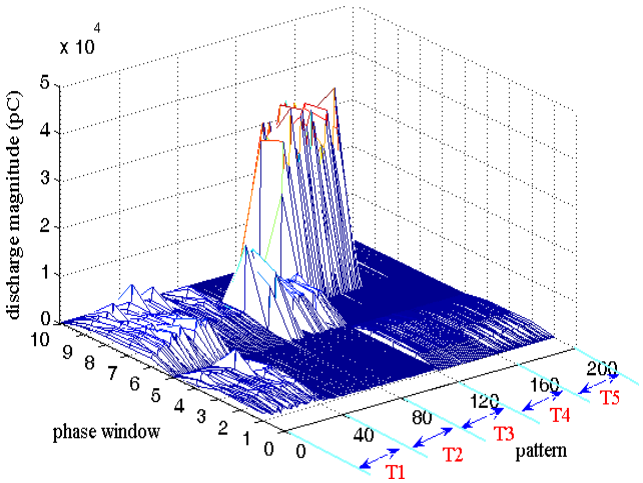

Fig.13 Mean discharge magnitude in phase windows

5.3 Recognition Accuracy of the Proposed Extension Rcognition Method

The diagnosis man-machine interface based on extension theory is shown in Fig.14. It consists of three parts. Part 1 is data input. We can directly input the features c1~c12. Part 2 is the defect type output recognized by extension theory. If the output of T2 is 1 then the defect type belongs type 2. Part 3 is the recognize rate with average of 10 random trials for all testing date which add noise to 30%.

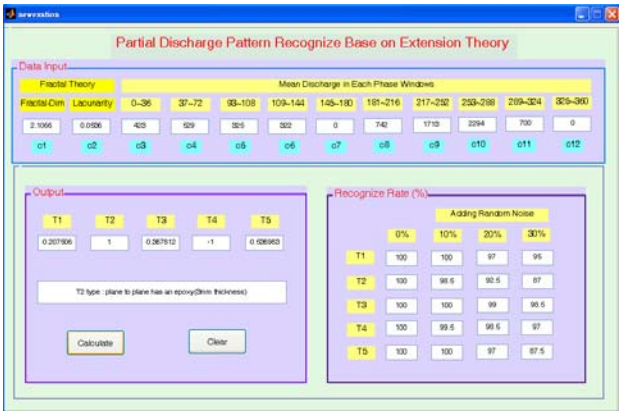

Fig.14 The diagnosis man-machine interface

Table 1 shows partial results of the proposed PD recognition system based on extension theory. It very clearly recognizes the defect type of tested models. For example, in pattern No 35, the index of correlation with the defect type 1 is equal 1(the max value), which indicates recognition result is T2. In comparison, the indices of correlation with other defect type are all negatives. Moreover, the proposed method can not only detect the main defect of the test object but also provide useful information for future trend analysis by the index of correlation. For example, pattern No 196 was recognized to have a main defect type of T5 due to the maximum index of

correlation. On the other hand, the index of correlation λ_2, about 0.76 also shows the result possibility belong type 2. This information will be most useful to find the hidden defects of models.

The input to a PD recognition system would unavoidably contain some noise. The sources of noise may be generated from the PD detector, environmental electromagnetic, or human mistakes, etc. To take into account the noise, 200 sets of testing data are created by adding the random uniformly distributed noise from ±10% to ±30% . The recognition accuracy rates with different amounts of noise added are given in Table 2. The recognition accuracy without noise added is 100% and even has 93% accuracy rate in the case of ±30% noise added. To demonstrate the effectiveness of the proposed method, comparative studies using a BPNN with 3 hidden layer and 12-12-5 neurons are conducted on the same testing data. The accuracy of the BPNN is only 83.8% in the same condition. It shows that the proposed method has a pretty high recognition accuracy and good tolerance to added noise. Moreover, the proposed recognition method does not need a learning process, but only finding the upperbound and lowbound of the input features. It is very encouraged to implement the proposed method in a PD detector device for real-time PD recognition.

Table 1 Partial recognition results

Pattern No	Correlation Index					Defect Type
	λ_1*	λ_2*	λ_3*	λ_4*	λ_5*	
35	1	-0.31	-0.33	-1	-0.82	T1
38	1	-0.18	-0.67	-1	-0.76	T1
62	-0.54	1	-0.35	-1	-0.68	T2
74	0.3	1	-0.15	-1	-0.65	T2
103	-1	-0.51	1	-0.99	-0.63	T3
107	-1	-0.25	1	-0.79	-0.43	T3
145	-0.63	-1	-0.26	1	-0.4	T4
153	-1	0.32	-0.55	1	-0.14	T4
196	0.12	0.76	-1	0.25	1	T5
200	-0.25	0.52	-1	0.54	1	T5

* λ_1 : Correlation index of defect 1.
* λ_2 : Correlation index of defect 2.
* λ_3 : Correlation index of defect 3.
* λ_4 : Correlation index of defect 4.
* λ_5 : Correlation index of defect 5.

Table 2 The accuracy rate of PD recognition

% of noise	The average recognition rate* (%)	
	Extension method	MNN
0%	100%	100%
± 10%	99.6%	98.5%
± 20%	96.8%	89.9%
± 30%	93%	83.8%

*: Average of 10 random trials.

6 Conclusion

This paper proposes a new PD recognition method based on the extension theory. The fractal features and the mean discharges are used to highlight the more detailed characteristics of the raw 3D PD patterns. The recognition rates of the proposed method are quite high with 93% in extreme noise of 30%. The experimental results indicate that this method is able to implement an efficient classification with a very high recognition rate. Compared with MNN method, the proposed method does not require particular learning processes and artificial parameters. In addition, the calculation of the proposed recognition algorithm is fast and very simple. This new method merits more attention to be a useful tool in PD recognition problems.

7 Acknowledgement

The research was supported by the National Science Council of the Republic of China, under Grant No. NSC 96-2213-E-167-029-MY3.

References

[1] J. Luo, H. Zhu, J. Feng, and J. Yuan, "Analysis of 3-d Partial Discharge Pattern in XLPE Power Cable Base on Fractal Theory," *IEEE International Symposium on Electrical Insulation*, April 2002, pp. 116-118.

[2] Z. Zhao, Y. Qiu, and E. Kuffel, "Application of Fractal to PD Signal Recognition," *IEEE International Symposium on Electrical Insulation*, April 2002, pp. 523-526.

[3] L. Jian, T. Ju, S. Caixin, L. Xin, and D. Lin, "Pattern Recognition of Partial Discharge with Fractal Analysis to Characteristic Spectrum," *International Conference on Properties and Application of Dielectric Materials*, Vol. 2, June 2000, pp. 21-26.

[4] T. K. A. Galil, R. M. Sharkawy, M. M. A. Salama, and R. Bartnikas, "Partial Discharge Pattern Classification Using the Fuzzy Decision Tree Approach," *IEEE Transaction on Instrumentation and Measurement*, Vol. 54, No. 6, December 2005, pp. 2258-2263.

[5] C. Mazzetti, F. M. F. Mascioli, F. Baldini, M. Panella, R. Risica and R. Bartnikas, "Partial Discharge Pattern Recognition by Neuro-Fuzzy Networks in Heat-Shrinkable Joint and Terminations of XLPE insulated Distribution Cables," *IEEE Transactions on Power Delivery*, Vol. 21, No. 3, July, pp. 1035-1044.

[6] H. Suzuki and T. Endoh, "Pattern Recognition of Partial Discharge in XLPE Cables Using a Neural Network," *IEEE Transactions on Electrical Insulation*, Vol. 27, No. 3, June 1992, pp. 543-549.

[7] R. Candela, G. Mirelli, and R. Schifani, "PD Recognition by Means of Statistical and Fractal Parameters and a Neural Network," *IEEE Transactions on Dielectrics and Electrical Insulation*, Vol. 7, No 1, February 2000, pp. 87-94.

[8] W. Cai, "The extension set and incompatibility problem," *Journal of Scientific Explore*, Vol. 1, 1983, pp. 81-93.

[9] S. S. Chen, J. M. Keller, R. M. Crownover, "On the Calculation of Fractal Features from Images," *IEEE Transaction on Pattern Analysis and Machine Intelligence*, Vol. 15, October 1983, pp. 1087-1090.

[10] L. Satish, W. S. Zaeng, "Can Fractal Features Be Used for Recognizing 3-D Partial Discharge Patterns? " *IEEE Transactions on Dielectrics and Electrical Insulation*, Vol. 2, June 1995, pp. 352-359.

[11] R. F. Voss, *Random Fractal: Characterization and Measurement*, New York, Plenum Press, 1985, pp. 1-11.

[12] B. B. Mandelbrot, *The Fractal Geometry of Nature*, New York, Freeman, 1983.

[13] M. H. Wang and C. Y. Ho, "Application of Extension Theory to PD pattern Recognition in High-Voltage Current Transformers," *IEEE Transactions on Power Delivery*, Vol. 20, No 3, July 2005, pp. 1939-1946.